



# Verification of the seismic P-wave velocities under Moho boundary: Central Poland case study, LUMP profile

Monika Dec<sup>1</sup> · Marcin Polkowski<sup>2</sup> · Tomasz Janik<sup>1</sup> · Krystyna Stec<sup>3</sup> · Marek Grad<sup>2</sup>

Received: 25 October 2017 / Accepted: 6 December 2018 / Published online: 13 December 2018  
© The Author(s) 2018

## Abstract

The tectonic settings investigated by several seismic projects in previous research targeting the structure in Central Poland mainly focused on the Earth's crust. In this paper, we present P-wave velocity verification in the uppermost mantle beneath LUMP profile towards SSE-NNW. Using recordings of 36 DATA-CUBE recorders from ca. 300–490 km far earthquake in coal mine “Janina” in southern Poland, we calculated travel times to verify P-wave velocity below the Moho boundary from previous studies. It shows that a significantly lower mean velocity value should be used for the upper mantle while counting these offsets of travel times in the SSE-NNW direction than that used on previous profiles. We present two possible models: first, the most simple one that fits the observed first arrivals, and the second with a low-velocity layer beneath the Moho boundary. In both cases, we used a priori crustal model focusing only on P-wave velocity in the uppermost mantle. Both of them significantly improved adjustment of travel times to the observed data. To evaluate the tendency of adopting too high velocities beneath the Moho, we used also 11 broadband stations, Reftek 151-121 “Observer”, from “13 BB Star” passive experiment and 6 STS-2 seismometers from permanent stations of the Polish Seismological Network (PLSN).

**Keywords** Upper mantle structure · Central Poland · P-wave velocity · Seismic profile

## Introduction

The tectonic structure in Poland, where the East European Craton and Palaeozoic Platform are divided by the Trans-European Suture Zone, is complicated (Fig. 1). The cross sections were modelled along relatively dense net of the seismic profiles in several projects, as, for example, POLO-NAISE'97 (e.g. Guterch et al. 1997), CELEBRATION 2000 (e.g. Guterch et al. 2003) or SUDETES 2003 (e.g. Grad et al. 2003). Figure 2 presents some of these profiles. The 2D models along particular profiles were the basis for creating 3D models by Majdański (2012) and Grad et al. (2016). These profiles were acquired during active source seismic experiments, where recorded energy is significantly lower than in case of natural earthquakes.

In 2015, there was an earthquake in the coal mine close to Libiąż town. At that time, we had a profile set up to record the energy from the detonation of one old sea mine with a total charge ca. 1700 kg of TNT from the FENNOLORA (1979) project (Lund et al. 1983). After almost 40 years since the FENNOLORA seismic experiment, the last unexploded military charge was detonated. All countries bordering the Baltic Sea were informed and set up their own equipment. Throughout the Scandinavian Peninsula, the energy from this blast was recorded (Lund 2015). Unfortunately, on the southern part of the Baltic Sea the energy from that blast was poorly recorded, probably because of the very bad weather conditions—strong wind and storm generating too much noise.

Deployment of stations at that time allowed us to record the mining event close to Libiąż town. The distance between the source and the receivers made it possible to verify P-wave velocity in the uppermost mantle in Central Poland. Assuming well-investigated crustal structures, we present an attempt to examine P-wave distribution below the Moho boundary or discontinuity based on Libiąż Uppermost Mantle Profile (LUMP profile). We used also recordings of all seismic stations deployed in Poland at that time (see Table 1).

✉ Monika Dec  
monikadec@igf.edu.pl

<sup>1</sup> Institute of Geophysics, Polish Academy of Sciences, Warsaw, Poland

<sup>2</sup> Faculty of Physics, Institute of Geophysics, University of Warsaw, Warsaw, Poland

<sup>3</sup> Central Mining Institute, Katowice, Poland

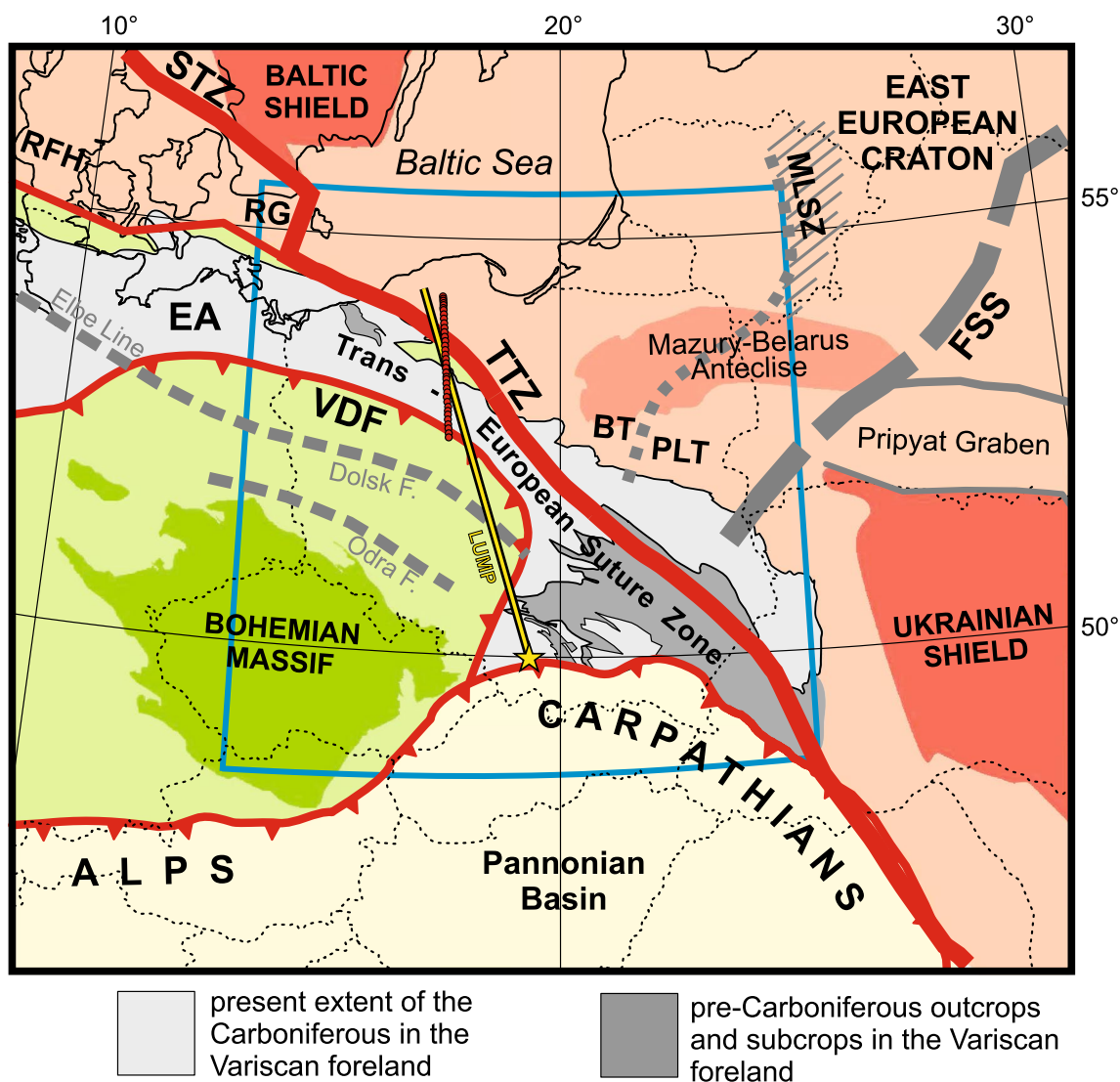


**Fig. 1** Tectonic sketch of the pre-Permian Central Europe in the contact of the East European Craton, Variscan and Alpine orogens compiled mainly from Pożaryski and Dembowski (1983), Ziegler (1990), Winchester et al. (2002), Skridlaitė et al. (2006), Cymerman (2007), Narkiewicz et al. (2011), Franke (2014) and Mazur et al. (2015). Blue frame shows the location of studied area. *BT* Baltic Terrane, *EA* Eastern Avalonia, *FSS* Fennoscandia-Sarmatia Suture, *MLSZ* Mid-Lithuanian Suture Zone, *PLT* Polish–Latvian Terrane, *RG* Rønne Graben,

*RFH* Ringkobing-Fyn High, *STZ* Sorgenfrei-Tornquist Zone, *TTZ* Teisseyre-Tornquist Zone, *VDF* Variscan Deformation Front. The area of Bohemian Massif is highlighted in dark green. The Trans-European Suture Zone separates thick and cold Precambrian crust from younger thin and hot Paleozoic crust. Yellow star shows the location of Libiąż earthquake which was recorded at LUMP seismic stations (red dots). Yellow line shows the LUMP profile

First, we present data-seismic waveforms from Libiąż seismic event. Second, we describe the methods used in this analysis (2D ray-tracing modelling). The modelling and results section presents two new models of the analysed region with seismic sections together with the travel times calculated for our models. Finally, we discuss the results.

## Tectonic settings

The LUMP profile line intersects three main tectonic units: the East European Craton in the north, Palaeozoic Plate in the south and the Trans-European Suture Zone that separates them (see Fig. 1).

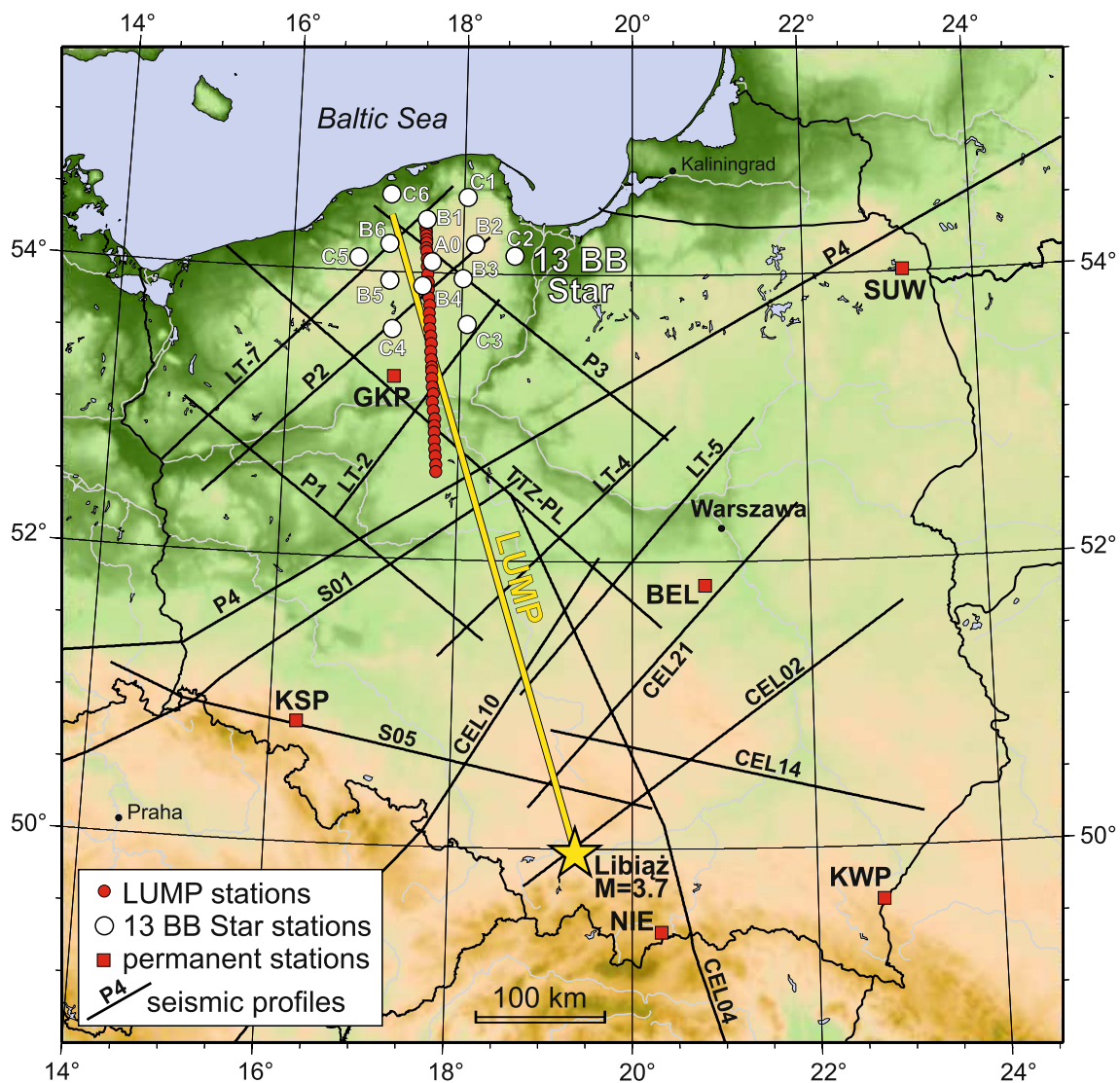


**Fig. 2** The net of selected profiles from the region neighbouring the LUMP profile on the background of the topographic map. Yellow star shows location of Libiąż earthquake which was recorded at LUMP seismic stations (red dots). “13 BB Star” array of broadband sta-

tions is denoted with white dots and permanent seismic stations with red squares, respectively. Yellow line shows the LUMP profile. Thin black lines are profiles used for the construction of the Model Z

The East European Craton (EEC) is the oldest part of Europe. It was formed around 1.8–1.7 billion years ago, due to the collision of three independent segments: Fennoscandia, Sarmatia and Volgo–Uralia (Bogdanova et al. 2001, 2005). There are metamorphic rocks of Archaean and Proterozoic age in the Precambrian platform, including plutonic and volcanic rocks, both alkaline and acidic. These are mainly migmatites, gneisses, amphibolites, granitic rocks and igneous rocks such as gabbros, syenites, granitoids, norites with a thick sediment coverage ~5 km on the SW rim, which gradually reduces its thickness towards the NE direction (Bogdanova et al. 2006; Puziewicz 2006; Puziewicz et al. 2017).

The Trans-European Suture Zone (TESZ) separates the young Paleozoic structures of Central and Western Europe from the old Precambrian structures of northern and eastern parts. This area was created as a result of the collisions of Baltica, Laurentia, Gondwana and Avalonia (Gee and Zeyen 1996). The western margin of East European Craton is the most prominent lithospheric border in Europe. It runs from north-west to south-east, from the North Sea to the Black Sea, at a length of about 2000 km. This zone of the Palaeozoic collision of the Precambrian East European Craton with the micro-continents of Avalonia, Barrandian and Armorica (which broke off from Gondwana in the south) is almost hidden in deep sedimentary basins from the Permian to the

**Table 1** List of seismic broadband stations

No.	Name	Lat (°N)	Lon (°E)	Elevation (m)	Distance from Libiąż event (km)
1	C3	53.64291	18.06823	121	406.9
2	B3	53.96410	18.00966	138	442.6
3	B4	53.90618	17.53553	137	444.2
4	B5	53.93703	17.14901	158	455.6
5	A0	54.07505	17.63717	165	460.4
6	B2	54.20622	18.14512	259	467.2
7	C5	54.11620	16.77978	119	482.9
8	B6	54.19633	17.13096	90	483.2
9	B1	54.37191	17.56642	120	493.6
10	C1	54.53468	18.04281	154	504.4
11	C6	54.53999	17.13336	61	519.4
12	NIE	49.4189	20.3131	649	101.0
13	BEL	51.8355	20.7888	173	221.1
14	KSP	50.8428	16.2931	353	232.7
15	KWP	49.6314	22.7075	448	247.1
16	GKP	53.2697	17.2367	115	384.4
17	SUW	54.0125	23.1808	152	511.4

Numbers from column 1 correspond to numbers of stations in Fig. 6. Stations are sorted according to increasing distance: 1–11, stations from 13 BB Star experiment, and 12–17, permanent PLSN stations. For their locations, see also Fig. 2

Cenozoic age. In the studies of the history of this region, many seismic experiments and drilling holes are helpful. This border is also present in the upper mantle (e.g. Babuška et al. 1998; Wilde-Piórko et al. 2010).

## Previous seismic studies

Geophysical research in this area consists mainly of seismic methods. Numerous profiles (Fig. 2, Table 2) were recorded in both the eastern and western parts of TESZ (e.g. Guterch et al. 2010). Seismic projects, such as the LT profiles in Poland (Guterch et al. 1986), TTZ-PL (Grad et al. 1999), POLONAISE'97 (Guterch et al. 1999), CELEBRATION 2000 (Guterch et al. 2003) and SUDETES 2003 (Grad et al. 2003), provided information on crustal structure for the East European Craton and neighbouring areas. These projects provided a large number of crustal structure images down to the Moho boundary, but only in a few cases there were deeper interpretations (Grad et al. 2002). During deep seismic soundings, some upper mantle phases, both reflected and refracted, were traced on up to distances of 400 km (POLONAISE'97, Grad et al. 2002).

In 1997, the POLONAISE'97 project (Polish Lithosphere Onsets-An International Seismic Experiment) was

**Table 2** Seismic profiles crossing LUMP profile and in its vicinity, sorted from the north to south

Name of the profile	Year	Length of the profile (km)	Experiment	Crossing distance at LUMP profile (km)	References
P3	1997	300	POLONAISE'97	503	Środa and POLONAISE Working Group (1999)
LT-7	1987 and 1992	560	LT-7	492	Guterch et al. (1994)
P2	1997	300	POLONAISE'97	434	Janik et al. (2002)
LT-2	1974	220	LT-2	370	Guterch et al. (1986), Grad et al. (2005)
TTZ-CEL03	1993 and 2000	740	TTZ-PL and CELEBRATION 2000	317	Grad et al. (1999), Janik et al. (2005)
P4	1997	800	POLONAISE'97	294	Grad et al. (2003)
S01	2003	630	SUDETES 2003	264	Grad et al. (2008)
LT-4	1977	255	LT-4	200	Guterch et al. (1986), Grad et al. (2005)
CEL10	2000	720	CELEBRATION 2000	136	Hrubcova et al. (2008), Grad et al. (2009a), Janik, not published
LT-5	1979	300	LT-5	125	Guterch et al. (1986), Grad et al. (2005)
CEL14	2000	300	CELEBRATION 2000	91	Środa et al. (2006)
CEL21	2000	320	CELEBRATION 2000	49	Janik et al. (2009)
S05	2003	440	SUDETES 2003	38	Janik, model under preparation
CEL02	2000	400	CELEBRATION 2000	9	Malinowski et al. (2005)
CEL04	2000	630	CELEBRATION 2000	Parallel	Środa et al. (2006)
P1	1997	300	POLONAISE'97	Parallel	Jensen et al. (1999)

conducted, aiming to study the lithosphere structure within the TESZ and the south-western part of the East European Craton (Guterch et al. 1999). Profile P4, which had its origin in SE Germany, passed through Poland and ended in Lithuania, was the longest POLONAISE'97 profile. Its length was about 900 km. Modelling of this area shows a visible change in the depth of the Moho from 30 km on the Palaeozoic platform to ~45 km under the TESZ and 40–50 km below the East European Craton.

Another project on a similar scale was CELEBRATION 2000 (Central European Lithospheric Experiment Based on Refraction). The total length of the profiles was 8900 km, with 147 shots (Guterch et al. 2003). The longest profile (1400 km) CEL05 crossed tectonic units of the EEC, the TESZ, the Carpathians and the Pannonian Basin. Modelling of this profile was initially based on the inversion of first arrivals only (Guterch et al. 2003), but later ray tracing was used (Grad et al. 2006). In the area of the EEC, a three-layer crustal structure was established. The CEL03 profile was a prolongation of previous TTZ-PL profile, jointly ~720 km long. The profiles run along the TESZ. Analysis of this profile has shown that the TESZ is not homogeneous. Several smaller units were separated within it (Janik et al. 2005). The depth of the Moho boundary varies from ~30 km in the Baltic Sea to ~50 km at the Ukrainian border.

In 2006–2008, the PASSEQ project was conducted, which provided further important data for detailed investigation of the upper mantle structure around the TESZ region in Central Europe (Wilde-Piórko et al. 2008). One of its results is a model of P-wave velocity variations with  $\pm 3\%$  in relation to the *iasp91* velocity model around the TESZ (JanuYTE et al. 2015). Using the TELINV nonlinear teleseismic tomography algorithm to perform the inversions, the seismic lithosphere–asthenosphere boundary (LAB) was found to be more distinct beneath the Phanerozoic part of Europe than beneath the Precambrian part.

The TESZ area was investigated previously in projects such as EUGENO-S (e.g. EUGENO-S Working Group 1988), EGT (European Geotraverse; e.g. Blundell et al. 1992) and BABEL (Baltic and Bothnian Echoes from the Lithosphere; BABEL Working Group 1993). Recent years show great interest in this area. Projects such as POLONAISE'97, CELEBRATION 2000 and SUDETES 2003 provided 2D and 3D models of seismic wave velocity based on deep seismic probes. These models illustrate the crust structure in the TESZ region, but the depth range of the models does not allow for precise determination of the upper mantle structures.

The crustal structure of the EEC is characterized by a thin sedimentary cover, of up to 2 km, and consists of three layers. The top crystalline layer has seismic P-wave velocities of 6.0–6.4 km/s, mid-layer of 6.5–6.8 km/s and lower layer of 6.8–7.2 km/s. The Moho boundary lies here at a

depth of 43–50 km (Grad et al. 2006). Towards the TESZ, the seismic structure is composed of a sedimentary layer of 9–12 km with P-waves of less than 5.4 km/s. Beneath, there is a consolidated upper crust (basement) at a depth of 15–20 km with P-wave velocity less than 6 km/s, middle crust with velocities of 6.3–6.6 km/s and lower crust with Vp values of 6.8–7.2 km/s.

The results of deep seismic surveys show how complex the structure of the Earth's crust is in this area. These soundings also point out differences in physical characteristics, which correspond to their differences in geological structure. Analysis of the results of these projects allowed, for example, to designate the Moho depth map (e.g. Grad et al. 2009b).

## Seismic data and Libiąż event

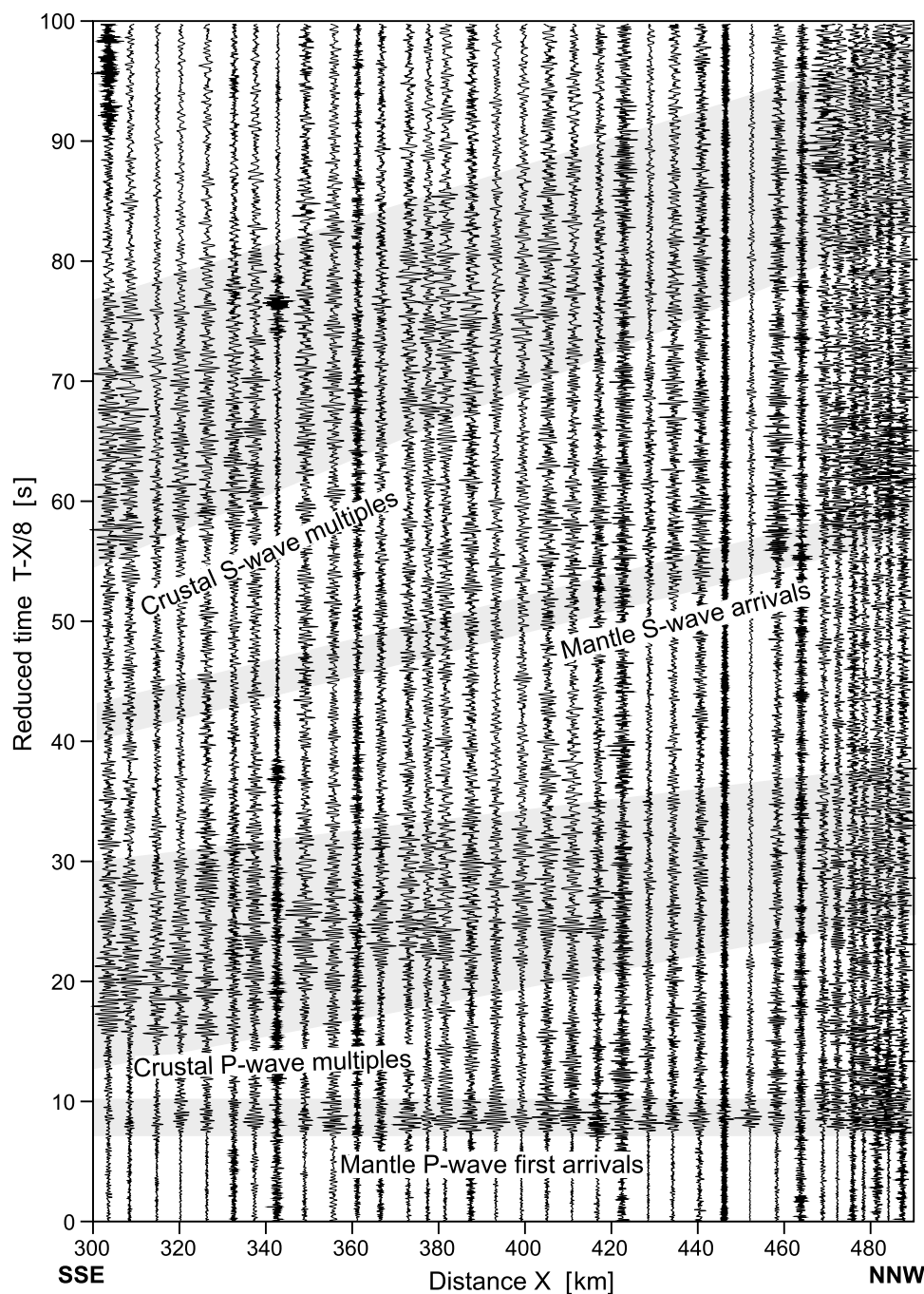
In this analysis, we used 36 short-period DATA-CUBE recorders, 11 broadband stations, Reftek 151-121 “Observer”, from “13 BB Star” passive experiment (Grad et al. 2015) and 6 from permanent broadband stations of the Polish Seismological Network (PLSN) equipped with STS-2 seismometers (locations in Table 1). Map of the LUMP seismic profile (yellow line) with all stations is shown in Fig. 2. DATA-CUBE recorders with 4.5 Hz geophones were deployed for 1 week only.

We used the source location catalogue with data calculated from mining seismometers (<http://www.grss.gig.eu/pl>), according to which the event occurred in 50.0717 N, 19.3396 E at the 1 km depth.

Seismic section composed of short-period data is presented in Fig. 3. Stations along the LUMP profile were deployed from 52.61220 N, 17.74969 E to 54.31169 N, 17.54922 E with average spacing 5.3 km. At 300–490 km offsets, we observed uppermost mantle seismic waves. The largest amplitudes are observed for first P-wave arrivals. We notice strong crustal P-wave multiples, but due to the complicated structure above the Moho discontinuity, attributing them to individual layers in the crust could be difficult. We recorded data on one-component DATA-CUBE with 100 cps, and on vertical component, we do not observe significant first-mantle S-waves. Trying to establish their position in Fig. 3, we mark a grey zone for approximately  $V_p/V_s \sim 1.73$  for both S-waves and crustal S-waves multiples.

To describe the source and energy radiation, we present moment tensor solution (Fig. 4). The “Janina” mine is located in Main Trough, the most extensive structure of Upper Silesian Coal Basin (USCB) (Buła et al. 2008; Bukowska 2012). It is a very gentle and extensive syncline with layer dip from 0° to 10°. Its main structural elements include a number of faults of varying amplitude of throws, often above 1000 m, and mild bending of layers in the form of domes, anticlinal faults or troughs and synclines. The

**Fig. 3** Seismic section recorded in northern Poland by LUMP stations (see Fig. 2 for location). Normalized Z-component, filtration 0.5–9.0 Hz



faults are mostly of regular throw and throw-slip kind, rarely only slip. The length of fault zones is not equal and ranges from a few metres to several dozen kilometres. Similarly, the orientation of faults varies from the latitudinal faults to the meridian; the latitudinal faults are characterized also by substantial throws, accumulated mainly in the central and southern part of the trough. Due to the fact that they throw rock mass to the south, the structure of the throw is stepwise, whereas the meridional faults are located almost all over the

area, and the NW–SE faults could be found only along the NE and E border.

The strong seismic event of  $M_L = 3.7$  occurred on November 11, 2015, during the coal seam 207 exploitation in “Janina” mine in Libiąż, southern Poland. In Fig. 4 we present the source mechanism of Libiąż seismic event which was determined from records of 11 channels of local “Janina” mine network. They were in the distance range of 300–490 m from the source and covered the azimuthal range quite well. In Fig. 4 they are projected into the focal sphere,

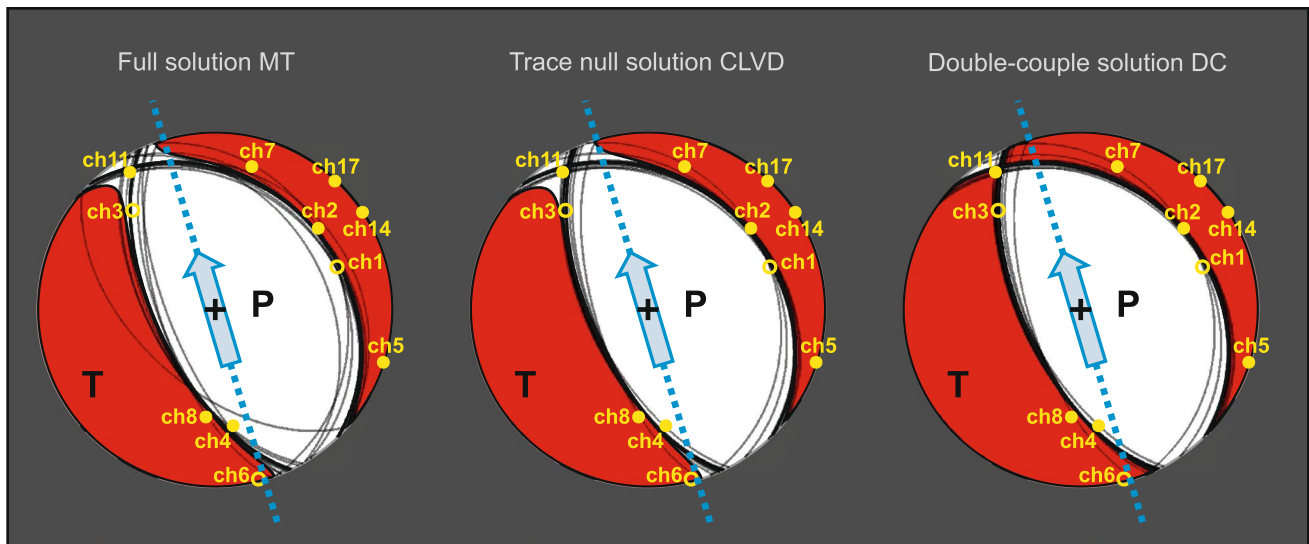


**Fig. 4** Source mechanism of Libiąż seismic event with a location of 11 channels of the local seismic network (“Janina” mine) used for moment tensor solution. They are at a distance of 310–1500 m from the source and cover the azimuthal range quite well. In this figure, their locations are projected into the focal sphere. The blue arrows show the direction to central stations at the LUMP profile (azimuth 343°). For this direction, mostly P-wave energy is generated, while the S-wave energy is much smaller which explains weak S-waves

and the blue arrows show the direction to central station of the LUMP profile.

For the analysed seismic event, the focal mechanism was calculated with seismic moment tensor inversion method (SMT) in the time domain from amplitudes and polarity of P-wave (Fig. 4). The SMT analysis was based on the seismograms recorded by underground seismic network in “Janina” mine. At the time of the event occurrence, the seismic network consisted of nine vertical and three three-component short-period (1–200 Hz) DLM3D seismometers manufactured by Central Mining Institute, with sampling rate of 500 cps. The recording seismometers are horizontally and vertically spaced from the seismic events at distance ranges of 0.4–3 km and 0.1–0.8 km, respectively.

The inversion was performed using FOCI 3.1.24 software (Kwiatek et al. 2016), applying constant velocity and density of 4.00 km/s and 2300 kg/m<sup>3</sup>, respectively. As a result of the calculations, three solutions were obtained following the convention introduced by Knopoff and Randall (1970):

- The full moment tensor, which can be decomposed into an isotropic component (ISO) describing the volume change, linear vector dipole (CLVD) and into the double-couple component (DC).
- The deviatoric tensor, containing a CLVD component and the shear component DC.

recorded at profile. **a** Full solution MT. The full moment tensor, which can be decomposed into an isotropic component (ISO) describing the volume change, linear vector dipole (CLVD) and into the double-couple component (DC) corresponding to the shear motion. **b** Trace null solution CLVD. The deviatoric tensor having a CLVD component and the shear component DC. **c** Double-couple solution (DC). The pure shear tensor, which has only the double-couple component (DC)

- The pure shear tensor, which has only the double-couple component (DC).

Figure 4 shows the parameters of the focal mechanism. The full, deviatoric and pure shear moment tensor was calculated using the L2 norm which was a measure of the misfit together with the Lagrange multipliers method (Wiejacz 1991).

The full moment tensor solution presented in Fig. 4 shows that the earthquake occurred as normal faulting on a north-west-striking plane. It is consistent with approximate strike local fault. Nodal plane A (trend  $-155^\circ$ , dip  $-63^\circ$ ) is almost vertical and plane B (trend  $-316^\circ$ , dip  $-27^\circ$ ) almost horizontal. High double-couple component of the moment tensor solution, which in here is almost 95%, confirmed that the probable cause was the effect of tectonic zones disturbed by mining activity.

## Modelling and results

### First check of data with 3D model

To compute seismic travel times with 3D seismic velocity model of Poland, the “pySeismicFMM” software package was used. The “pySeismicFMM” is Python-based travel

time calculation software in regular 2D and 3D grids in geographic and Cartesian coordinates. For given geographic coordinates of seismic source within the model, “pySeismicFMM” calculates travel times to all grid cells of the model in single pass, providing accurate travel time to any geographic coordinate within the model. The program uses the fast marching method (Sethian 1996; Sethian and Popovici 1999).

The 3D P-wave velocity model Grad et al. (2016) was obtained by combining data from studies from past 50 years and used data sources such as refraction and reflection seismology, vertical seismic profiling, geological boreholes, magnetotellurics and gravimetry. Such numerous data sources allowed to create detailed 3D P-wave velocity model which reaches to a depth of 60 km. It includes six layers of sediments, three layers of the crust and a single layer of uppermost mantle. The model grid covers a whole area of Poland from topography to 60 km depth. This model was calculated in a rectangular grid in geographic coordinates.

Each grid cell is assigned to one of the layers. A single grid cell has size of 1112 m × 1281 m × 10 m for northern Poland and 1112 m × 1459 m × 10 m for southern Poland. More detailed information can be found in Grad et al. (2016).

We used this model as a starting model in our study. In Fig. 5a we present the vertical cross section obtained from this 3D model between Libiąż location and the middle point of the LUMP profile. Seismic sections (Fig. 5b) with travel times calculated for the 3D model show that the fit to the data should be improved. The root mean square (RMS) value for this model is 0.924 s with picking accuracy 0.1 s. All source–receiver seismic rays penetrate the uppermost mantle. Tracing wave propagation, we notice that due to the distance, only the part of the model beneath the Moho could be slightly corrected.

Although P-wave penetration is not deep enough (down to ~ 10 km below the Moho) to evaluate seismic velocities, we noticed that uppermost values are too high. Propagation of P below the Moho begins at a relatively high velocity,

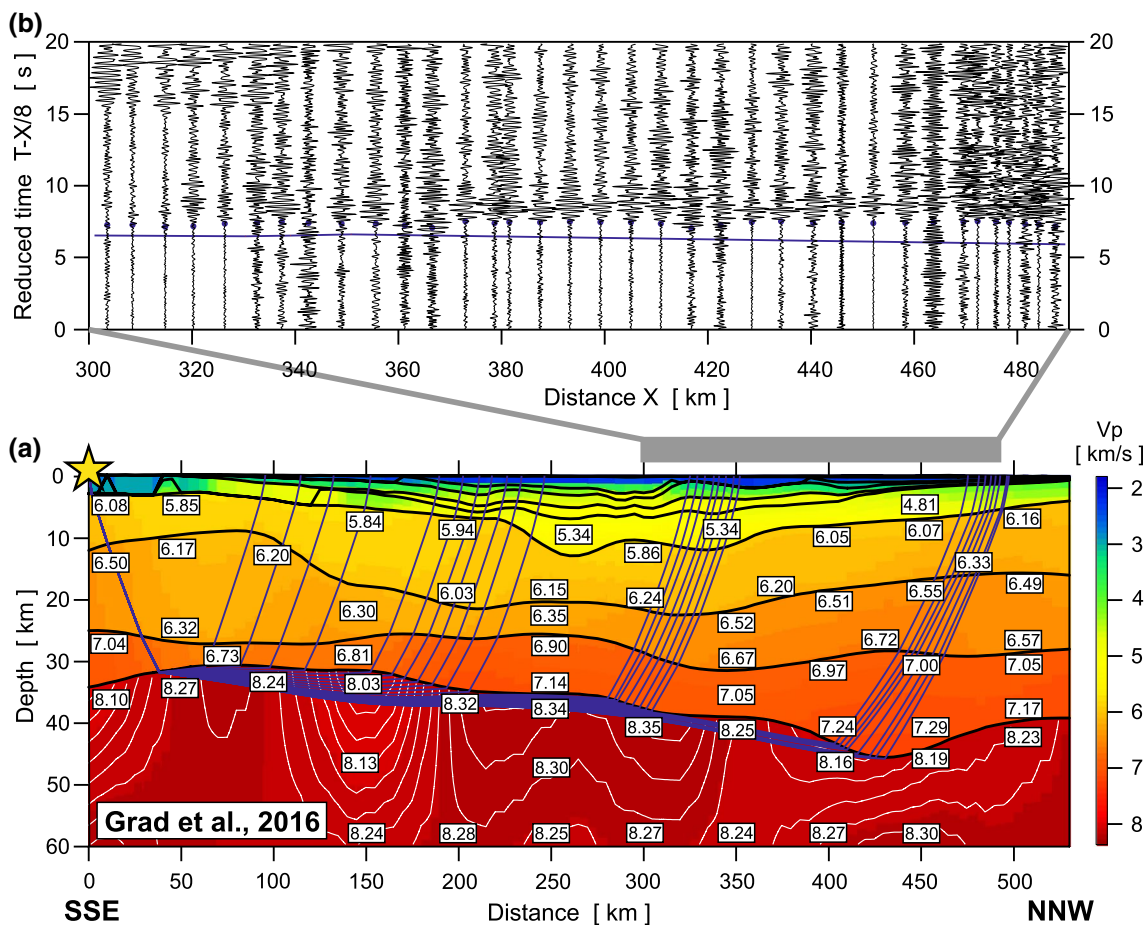


**Fig. 5** **a** Vertical cross section obtained from 3D model of P-wave velocity in Poland (Grad et al. 2016) between the event location and middle point of the LUMP profile. Thick, black lines represent velocity discontinuities (interfaces). Velocity values in km/s are shown in

white boxes. Thin, white lines represent velocity contour lines (each 0.03 km/s). Blue lines correspond to ray paths. **b** Seismic sections with travel times calculated for the 3D model (blue line). Normalized Z-component, filtration 1.5–6.0 Hz. Blue dots represent first arrivals



with  $\sim 8.27$  km/s at  $\sim 50$  km distance. This value decreases down to  $\sim 8.03$  km/s at distance  $\sim 150$  km. In the middle of the LUMP, there are high P velocities at distances from 190 to 350 km with  $\sim 8.34$  km/s at 250 km and  $\sim 8.36$  km/s at 300 km. This “island” with high velocities is characterized by negative gradient of P velocities. Further along the profile, at a distance above 350 km, P velocity values decrease again, down to  $\sim 8.16$  km/s at 400 km.

Difference between observed and theoretical travel times from 3D model is mainly caused by model inaccuracy. Differences between blue line and blue dots (Fig. 5b) can be characterized by  $RMS = 1.12$  s.

Because rays mostly travel through the uppermost mantle, the influence of P-wave velocity modification on travel time fit was tested for all stations (LUMP + “13 BB Star” + PLSN). Figure 6 (with legend in Table 1) shows absolute travel time difference (colour scale) for different uppermost-mantle velocity modifications (UMM velocity factor; vertical scale, from +3% in the bottom, to  $-7\%$  on top) for each station (horizontal scale, one column per station, stations sorted by distance from source, separately for each station group). White dots show velocity change providing the best time fit for each station. Seismic wave from source to closest PLSN station (NIE) did not propagate in the uppermost mantle, so for this station travel time accuracy does not change with modification of the uppermost mantle velocity.

Although seismic records from 13BB and PLSN presented in Fig. 6 do not help with modelling along the LUMP profile, they were used in general for 3D model verification. We cannot assume that the model of Grad et al. (2016) has too high P-wave velocities below the Moho for other directions of wave propagation. To exclude the fact that these velocities are too high for the whole model, we show that for PLSN for two stations its values are too small and for one station the travel time difference is really small.

### Testing $V_p$ in the lower lithosphere

For modelling of the P phase, we used travel time inversion, which is a commonly used method that allows to reconstruct seismic velocity model basing on the observations of the arrival times of seismic phases. In this paper, we used the Rayinvr program (Zelt 1999) modified by Gorman (2002). This program assumes isotropic, two-dimensional medium, consisting of layers with smoothly varying P-wave velocities, with possible velocity discontinuities at the layer boundaries. The velocity in each layer is parameterized on a trapezoidal grid at user-defined nodes, with linear interpolation between neighbouring nodes to obtain the velocity field at any point of the model. As an initial model, usually a simple 1D velocity field is used. For the calculation of travel times and ray paths (ray theory approximation), numerical

solution of eikonal equations for two-dimensional media by the Runge–Kutta method is performed. Differences (residuals) between the observed travel time data and travel times calculated for the current model represent the input for linearized damped least squares inversion procedure. Inversion results in corrections of the velocity model that improve the fit to the observed data. Usually, several iterations of the inversion and of model corrections are needed, and inversion is stopped when RMS travel time residual is on the level of estimated data (picking) errors.

Using this tool we estimated a new P-wave velocity model for the LUMP profile (Fig. 7a). We assumed crustal velocities after Grad et al. (2016) as it is shown in Fig. 5a. Tracing P-wave propagation, we focused only on the uppermost mantle below Moho. To analyse model incompatibilities, we create a new model using 2D forward seismic modelling with starting Model X which had velocity from 8.05 km/s just beneath the Moho to 8.17 km/s at the depth of 60 km (Fig. 7b), which significantly improved the propagation of deep rays. Model X was used as a starting model in inversion analysis.

In order to limit the ambiguity of the solution, the velocities in the crust and the Moho depth were assumed to be known based on 3D well-documented model and were not subject to inversion. Therefore, only the uppermost mantle velocities were modelled. The velocities were parameterized in nodes with  $\sim 5$  km step. In general, with a single source, the ray distribution is unfavourable for inversion, but as ray paths in the modelled layer have different length, they still provide some independent information. Therefore, we decided to use such a simple inversion procedure to evaluate the mantle velocities.

After three steps of inversion, we obtain Model Y (Fig. 7a). Accuracy of fitting the data is shown in Fig. 7c. The RMS value after inversion is 0.23. Model Y has two areas with relatively higher P-wave velocity,  $\sim 8.16$  km/s at 275 km and  $\sim 8.15$  km/s at 380 km, and two with lower,  $\sim 7.90$  km/s at 350 km and  $\sim 7.95$  km/s at 400 km (Fig. 7b). P-wave velocity is significantly lower than that in the model of Grad et al. (2016). This change improved coverage of rays propagation in the uppermost mantle. (Earlier crossing profiles have higher P-wave velocity in the uppermost mantle.)

### Trial-and-error forward modelling

Based on data from intersections with 14 wide-angle reflection and refraction profiles conducted earlier, a velocity distribution model of P-waves, here model Z (Fig. 8a), was constructed along the LUMP profile (Fig. 2). Since the construction of Model Z includes slightly more or different data variants, as well as another interpolation method, in some details this model differs from the models presented

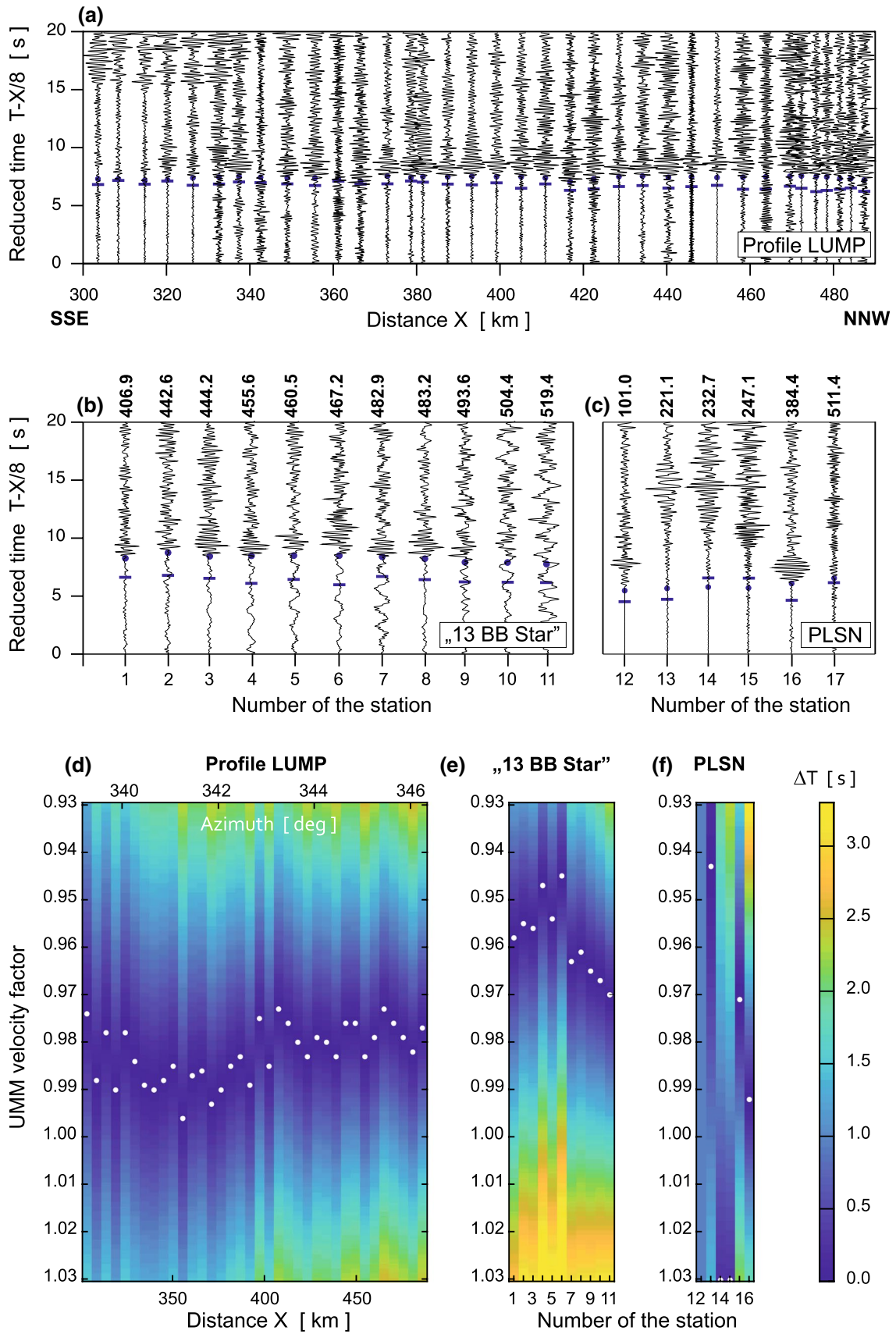


**Fig. 6** Seismic section with travel times calculated with the 3D model (blue dashes) and first arrivals (blue dots) for **a** the LUMP profile, filtration 1.5–6.0 Hz, **b** 13BB Star, filtration 0.5–6.0 Hz, **c** PLSN stations, filtration 1.5–6.0 Hz. Differences between observed and theoretical travel time from 3D model for: **d** the LUMP profile, **e** 13BB Star, **f** PLSN stations

earlier (Model X and Model Y). Taking into account the complexity of data from so many profiles crossing the LUMP profile from different angles, it is possible to understand the complexity of the crustal part of the model. This is an alternative model to presented earlier Model Y (Fig. 7a). In the modelling process, the crustal part of the model was frozen (assumed to be constant), as well as the shape of the Moho boundary. The Moho depth changes along the model from about 32 km in SSE to 42 km in NNW. Beneath many profiles crossing TESZ, we observe a very well-documented high-velocity  $V_p$  under the Moho boundary; for example, on TTZ-PL profile  $V_p$  is  $\sim 8.4$  km/s (Grad et al. 1999; Janik et al. 2005). On profiles which cross the LUMP profile at a greater angle, the velocities are similar or slightly lower: CEL02  $\sim 8.25$  km/s (Malinowski et al. 2005); S05  $\sim 8.35$  km/s (Janik, under preparation); CEL21  $\sim 8.4$  km/s (Janik et al. 2009); CEL14  $\sim 8.4$  km/s (Środa et al. 2006); LT-5  $\sim 8.35$  km/s (Guterch et al. 1986; Grad et al. 2005); CEL10  $\sim 7.9$  (8.2) km/s (Hrubcova et al. 2008; Grad et al. 2009a; Janik, not published); LT-4  $\sim 8.35$  km/s (Guterch et al. 1986; Grad et al. 2005); S01  $\sim 8.35$  km/s (Grad et al. 2008); P4  $\sim 8.4$  km/s (Grad et al. 2005). In the northern part of the model, where the profile enters the EEC, observed  $V_p$  velocities are slightly lower: LT-2  $\sim 8.1$  km/s (Guterch et al. 1986; Grad et al. 2005); P2  $\sim 8.15$  km/s (Janik et al. 2002); LT-7  $\sim 8.2$  km/s (Guterch et al. 1994); P3  $\sim 8.05$  km/s (Środa and POLONAISE Working Group 1999).

The crustal part of Model Z, as well as the shape of the Moho boundary, was assumed to be constant in the modelling process. Only the velocities in the uppermost mantle were modelled. The trial-and-error forward modelling was carried out with the SEIS83 package (Červený and Pšenčík 1984) together with its graphical interface model (Komminaho 1998) and ZPLOT software (Zelt 1994). In the first step, the P-wave computed with  $V_p \sim 8.4$  km/s for the whole uppermost mantle, arrived approximately 1.0 s earlier than the recorded signals, similar to the model of Grad et al. (2016) presented in Fig. 5b. Modifications of the uppermost mantle tested in many subsequent steps of the trial-and-error modelling led to the model shown in Fig. 8a. Just below the Moho, up to  $\sim 330$  km of the Model Z, there is a layer of thickness 4–12 km and  $V_p \sim 8.25$ –8.3 km/s. This value is slightly lower than that suggested by the intersected profiles, but more similar to the  $V_p$  occurring on CEL04 profile ( $V_p = 8.1$ –8.35 km/s, Środa et al. 2006) located near

parallel to the southern part of the LUMP profile (90–40 km to the east). This may indicate the presence of directional anisotropy in this layer. According to data from other profiles, at a distance of 330–505 km, the velocity in this layer is  $V_p = 8.05$ –8.1 km/s. Under this layer in the entire length of the Model Z, we assumed the existence of a layer with lower velocities. (In case of  $V_p$  of 8.0–8.1 km/s, its thickness should be  $\sim 17$ –20 km.) At a depth of about 55 km, another boundary was modelled, under which  $V_p > 8.35$  km/s. At distances of 170–350 km of the Model Z, this boundary is dipping into 70 km. Modifications were done to bring theoretical travel times into accordance with the correlations of the  $P_{\text{mantle}}$  wave observed on the recorded section on the LUMP profile, at offset between 300 and 490 km.

For searching S-waves travel times, we used Model Z obtained from P-waves, applying a  $V_p/V_s$  ratio individually for each layer. Due to the quality of the data we had, we limited ourselves to general modelling of the  $V_p/V_s$  ratio. Modelling assumed  $V_p/V_s = 1.73$  for the whole Model Z, except for the two deepest layers where  $V_p/V_s = 1.74$ . This allows us to show  $P_{\text{mantle}}$  together with expected  $S_{\text{mantle}}$  phases from below the last boundary in Model Z. The modelled travel times for both P- and S-waveforms are derived from phases multiple reflected from middle and/or lower crust penetrating the selected layers. In general, they fit quite well with the area of the amplitude increase observed in the seismic section.

Model Z is an alternative to Model Y presented earlier (Fig. 7a). Its assumptions are in line with the previously collected velocity information and the belief that under the TESZ there is a uniform high-velocity layer just beneath the Moho. Model Z contrasts with the Model Y, where just under the Moho we observe a huge lateral variation of the velocity values for P-waves.

## Discussion and conclusions

We raised the question: Are we able to draw important conclusions about the structure thank to such a small experiment as LUMP profile? The answer is: Yes, we are. We are aware of the fact that we only make the previous model more detailed but we show corrected  $V_p$  distribution below Moho in central Poland. By analysing the P-wave velocities in the uppermost mantle beneath the central part of Poland, beneath the models parallel to LUMP profile, we observe much lower values than we would expect from previous investigations in the region. In the first presented model (Fig. 5a) based on the velocity data set prepared by Grad et al. (2016), the values from 8.27 km/s at 50 km of the profile or 8.32–8.36 km/s in its central part do not fit the first arrivals on seismic section.

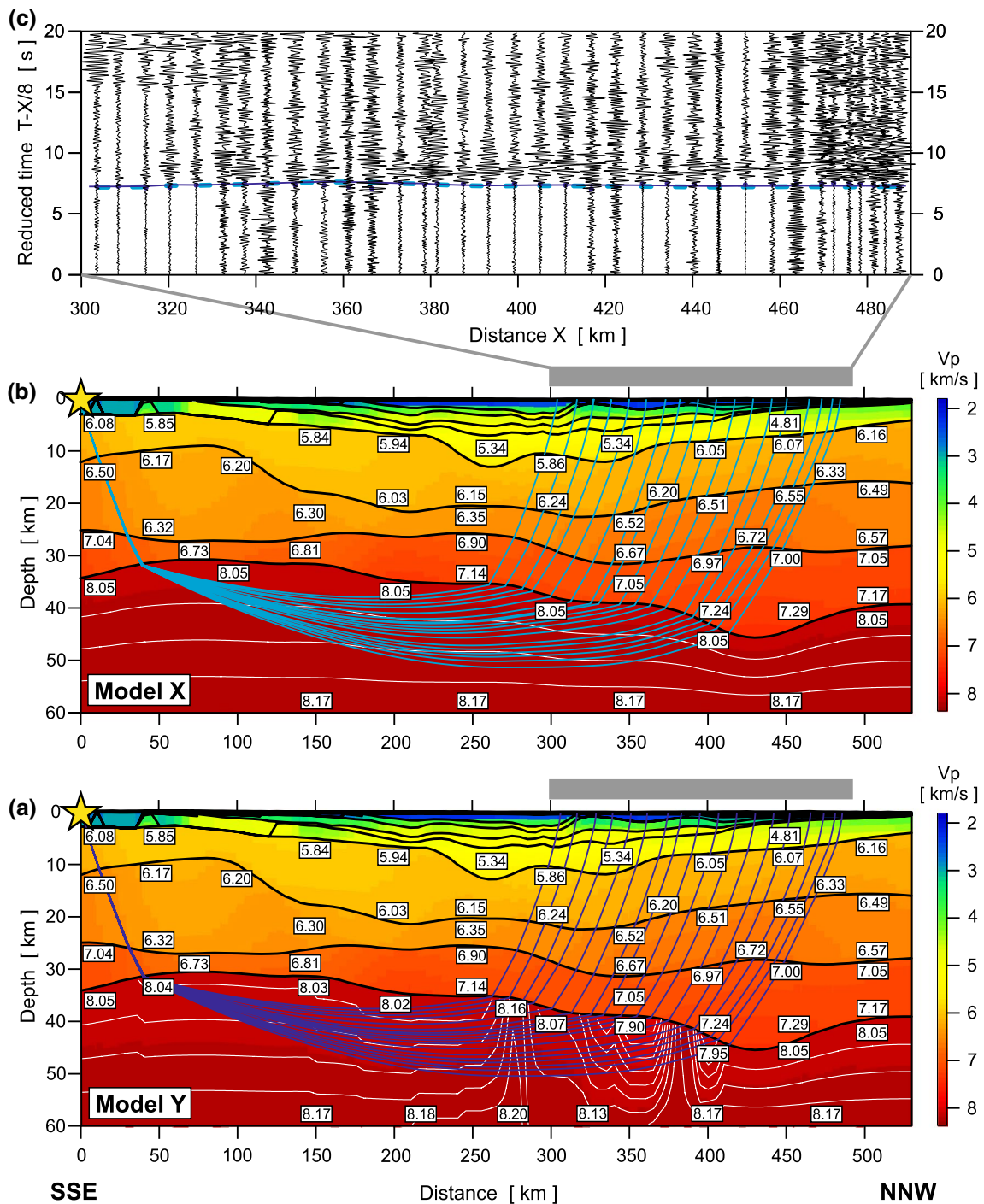


**Fig. 7** **a** The Model Y of the LUMP profile obtained by seismic inversion (Model Y). Thick, black lines represent velocity discontinuities (interfaces). Velocity values in km/s are shown in white boxes. Thin, white lines represent velocity contour lines (each 0.03 km/s). Blue lines correspond to ray paths. **b** The Model X—vertical cross section obtained from 3D model of P-wave velocity in Poland

between event location and middle point of the LUMP profile with Model X below the Moho discontinuity. **c** Seismic section with calculated travel times: navy blue line—for the new model presented in **a**; light blue dashed line—for model (**b**), and first arrivals (navy blue dots), filtration 1.5–6.0 Hz

Model X was composed using 2D forward seismic modelling and changing model beneath the Moho into one layer with  $V_p \sim 8.05$  km/s in the top and 8.17 km/s at 60 km

depth, which significantly improved travel times fit to the data (Fig. 7b). Optimizing this model by using inversion, we obtain the best results for Model Y with two higher

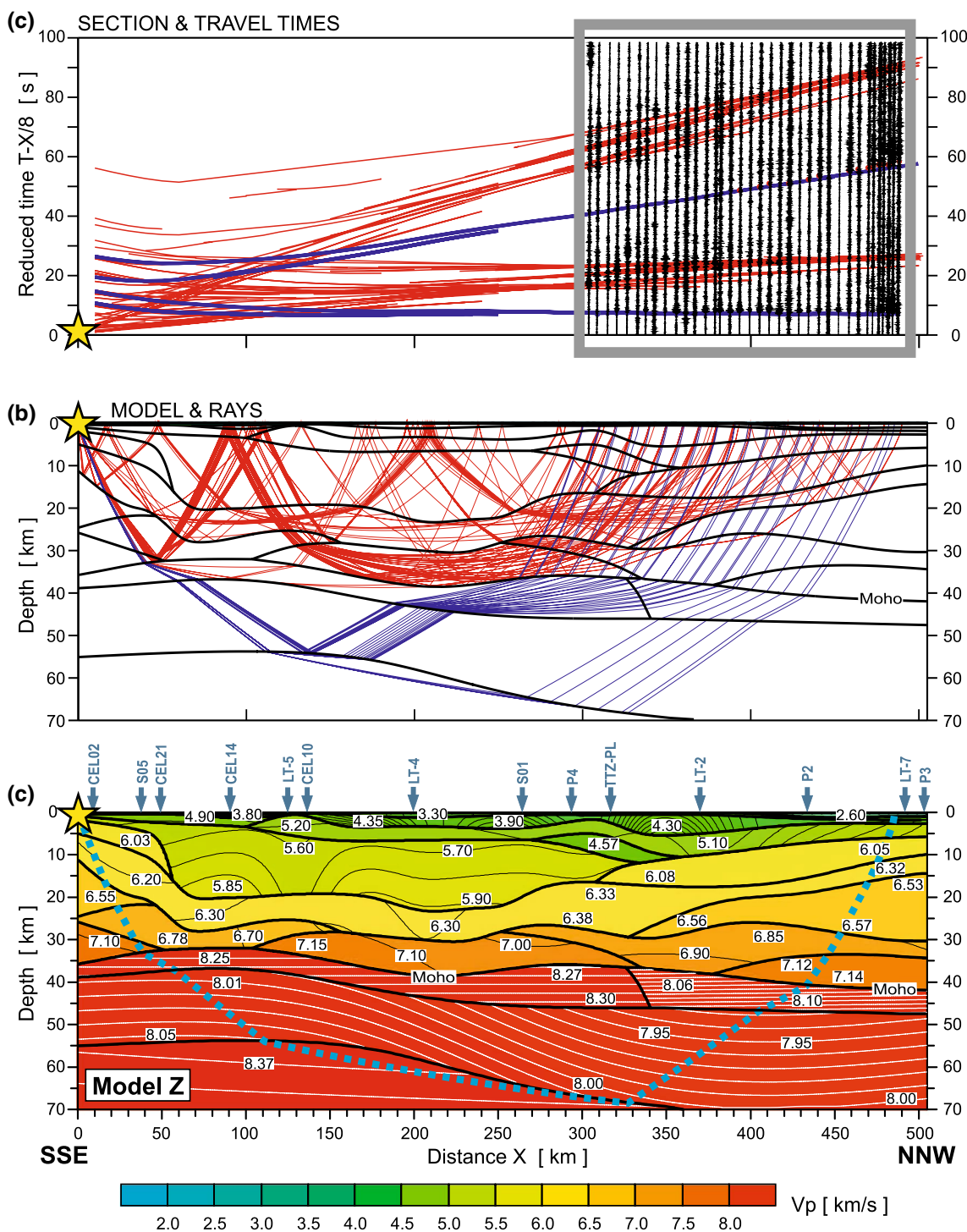


**Fig. 8** **a** The Model Z—2D ray-tracing P-wave velocity model for the LUMP profile. Please note that the crustal part of the model is constructed from models listed in Table 2, which cross the LUMP profile. Only velocities in the uppermost mantle were modelled. Thick, black lines represent velocity discontinuities (interfaces). Thin black lines represent velocity contour lines in the crust (each 0.1 km/s). Thin white lines represent velocity contour lines under Moho (each 0.01 km/s). Blue lines correspond to ray paths. Blue dashed line cor-

responds to the range of ray propagation. Velocity values in km/s are shown in white boxes. **b** The ray paths refracted and reflected at crustal uppermost mantle discontinuities with multiples. **c** Seismic sections with travel times calculated for the model presented in **a**. **d** Enlargement of seismic section from grey frame presented in Fig. 8c, filtration 0.5–9.0 Hz. Red rays on **b** red travel times on **c** and **d** diagrams represent selected crustal multiples which can explain high amplitudes after first arrivals. They are not included in modelling

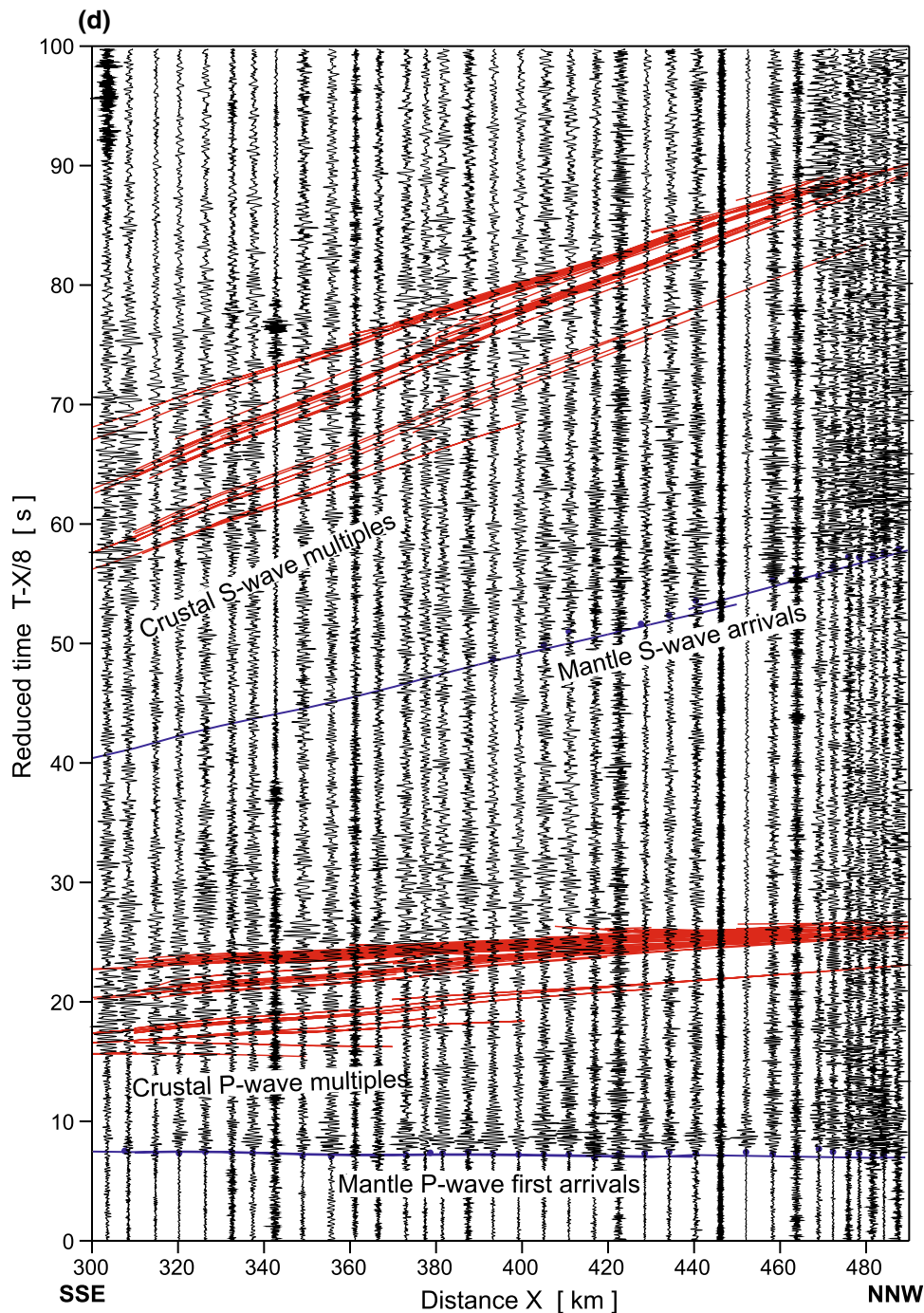


Fig. 8 (continued)

P-wave velocity areas, 8.16 km/s at 275 km and 8.15 km/s at 380 km, and two lower areas, 7.90 km/s at 350 km and 7.95 km/s at 400 km (Fig. 7a). This change also let rays to propagate deeper.

Both these solutions, “island nature” of high-velocity uppermost mantle and relatively low-velocity values, appear to be unrealistic as they essentially depart from the upper mantle structure presented on profiles that intersect

the LUMP profile. Not all of them have equal proof in data, but particularly the TTZ and P4 profiles have extensive areas of well-documented high-velocity upper mantle  $V_p \sim 8.25$  km/s and  $V_p \sim 8.4$  km/s, respectively. A similarly well-documented high-velocity area occurs on the P1 profile (Jensen et al. 1999). It is difficult to imagine that the LUMP profile just between them had so much lower velocity in the upper mantle. Considering this, a compromise

model was proposed. It assumes the existence of a high-velocity layer directly below the Moho boundary with  $V_p \sim 8.25$  km/s, which is the lowest of the high-velocity values observed on crossed profiles up to a distance of  $\sim 300$  km and  $V_p \sim 8.1$  km/s to the end of the profile. On the other hand, it was necessary to significantly delay the arrival times of theoretical travel times to match the times observed in our seismic section (Fig. 8c). In the trial-and-error modelling, many different variants of solutions were tested to achieve  $\sim 1$  s time delay effect of  $P_{\text{mantle}}$  wave. As a result, the solution presented in the Model Z in Fig. 8a was adopted. The uppermost mantle has three layers. The first two parts, directly under the border of the Moho, have a thickness of 4–12 km with  $V_p = 8.2\text{--}8.3$  km/s to about 330 km of profile and further with  $V_p = 8.04\text{--}8.12$  km/s. The P-wave running in this layer reaches maximum offset shorter than the observation interval of our seismic section. Postponed delay was achieved by adding 15–23 km-thick low-velocity zone beneath the first boundary (Fig. 8a) ( $V_p \sim 8.03$  km/s at the beginning of the profile,  $\sim 8.0$  km/s in the middle and 7.97 km/s at the end of the profile). Next layer which produces the observed  $P_{\text{mantle}}$  travel times requires higher velocities beneath this layer (8.37 km/s). To fit the data, this lower layer is observed at a depth of  $\sim 55$  km at a distance up to 150 km. It gently deepens up to a distance of  $\sim 350$  km to finally disappear at 70 km depth. Wave propagation cannot verify its existence at further distances.

Model Z, i.e. the 2D seismic forward model calculated for the LUMP profile, confirms that the existence of a relatively thin layer with  $\sim 8.25$  km/s P-wave velocity just below the Moho boundary is possible, but it requires lower velocity layer above next boundary with  $V_p \sim 8.37$  km/s at depths of 55–65 km. Due to the fact that there is a low-velocity zone, it is impossible to determine accurately its values. There is a possibility to assume a class of other solutions with thinner layers with lower P-wave velocity and changed depth of the deepest boundary, respectively. Previous profiles crossing the TTZ from SW to NE have indicated higher P velocity,  $\sim 8.4$  km/s (e.g. Guterch et al. 1994; Grad et al. 2003). Also teleseismic P-wave tomography results of PASSEQ data show lower P-wave velocity values to the west of the TESZ and higher ones to the east of it (Janutyte et al. 2015). Typically, the waves in the Precambrian lithosphere sections are considered to move faster than in their younger counterparts.

We claim that in the direction of the LUMP profile (SSE–NNW) the P-wave velocity should be reduced to  $\sim 8.1$  km/s beneath Moho or assuming higher velocities ( $\sim 8.25$  km/s, more consistent with velocities observed on crossing profiles), and there is a need to add a low-velocity zone below and a higher velocity layer ( $V_p \sim 8.37$  km/s) beneath it. Such a reduced P-wave velocity in the uppermost mantle can be explained by directional anisotropy. Another conclusion is

that there emerges a possibility of a more complicated upper mantle structure under the LUMP profile in the southern part of Poland than in previously accepted models, where P-wave velocities are not so well documented as in the northern part. Anyway, the analysis of these data shows how carefully and critically we have to consider the previously calculated 2D models as well as 3D models based on them (Majdański 2012; Grad et al. 2016), especially in the uppermost mantle. We have to take into account their imperfections (limited or not the best quality of data).

In this paper, we did not analyse details of S-wave velocity distribution. We assumed only  $V_p/V_s = 1.73$  for most of the model and  $V_p/V_s = 1.74$  for the two deepest layers. Relatively weak S-wave arrivals can be explained by the full moment tensor solution, which shows that the earthquake had normal faulting on a north-west-striking plane and very high double-couple component caused pure shear tensor.

The complex area has been studied repeatedly. The research projects were aimed at getting to know the geology and tectonics of the TESZ zone in different areas. The origin and further evolution of this area are still the subject of research and are still not yet fully understood, but every piece of information is verifying another structural fragment and should be added to previous/other research. New models of the uppermost mantle velocity do not change tectonic implications; however, the velocities should be corrected beneath the TESZ area. Such information is useful, for example, in petrological and gravimetric studies.

**Acknowledgements** Participation of the group from the Institute of Geophysics PAS in this work was supported within statutory activities No. 3841/E-41/S/2017 of the Ministry of Science and Higher Education of Poland and by National Science Centre in Poland—Grant DEC-2011/02/A/ST10/00284. Some of the presented figures were prepared with Generic Mapping Tool package (Wessel and Smith 1995). We would like to thank three anonymous reviewers whose comments significantly improved this paper.

**Open Access** This article is distributed under the terms of the Creative Commons Attribution 4.0 International License (<http://creativecommons.org/licenses/by/4.0/>), which permits unrestricted use, distribution, and reproduction in any medium, provided you give appropriate credit to the original author(s) and the source, provide a link to the Creative Commons license, and indicate if changes were made.

## References

- BABEL Working Group (1993) Deep seismic reflection/refraction interpretation of crustal structure along BABEL profiles A and B in the southern Baltic Sea. *Geophys J Int* 112:325–343
- Babuška V, Montagner JP, Plomerová J, Girardin N (1998) Age-dependent large-scale fabric of the mantle lithosphere as derived from surface-wave velocity anisotropy. *Pure Appl Geophys* 151(2):257–280
- Blundell D, Freeman R, Mueller S (eds) (1992) A continent revealed: the European Geotraverse. Cambridge, Cambridge University Press, p 275

- Bogdanova SV, Gorbatshev R, Stephenson RA (2001) EUROBRIDGE: Paleoproterozoic accretion of Fennoscandia and Sarmatia. *Tectonophysics* 339:7–10
- Bogdanova SV, Gorbatshev R, Garetzky RG (2005) The East European Craton. In: Selley RC, Cocks LRM, Plimer IR (eds) *Encyclopedia of geology*, vol 2. Elsevier, Amsterdam, pp 34–49
- Bogdanova S, Gorbatshev R, Grad M, Guterch A, Janik T, Kozlovskaya E, Motuza G, Skridlaite G, Starostenko V, Taran L, EUROBRIDGE, POLONAISE Working Groups (2006) EUROBRIDGE: new insight into the geodynamic evolution of the East European Craton. In: Gee DG, Stephenson RA (eds) *European lithosphere dynamics*, vol 32. Geological Society of London Memoirs, London, pp 599–625
- Bukowska M (2012) The rockbursts in the Upper Silesian Coal Basin in Poland. *J Min Sci* 3:445–456
- Buła Z, Żaba J, Habryn R (2008) Tectonic subdivision of Poland: southern Poland (Upper Silesian Block and Małopolska Block). *Prz Geol* 56:912–920 (in Polish, English summary)
- Červený V, Pšenčík I (1984) SEIS83-Numerical modelling of seismic wave fields in 2-D laterally varying layered structures by the ray method. In: Documentation of earthquake algorithms by ER Engdahl. World Data Center (A) for Solid Earth Physics, Report SE-35, pp 36–40
- Cymerman Z (2007) Does the Mazury dextral shear zone exist? *Prz Geol* 55:157–167 (in Polish with English abstract)
- EUGENO-S Working Group (1988) Crustal structure and tectonic evolution of the transition between the Baltic Shield and the North German Caledonides (the EUGENO-S Project). *Tectonophysics* 150:253–348
- Franke W (2014) Topography of the Variscan orogen in Europe: failed-not collapsed. *Int J Earth Sci* 103:1471–1499
- Gee DG, Zeyen HJ (eds) (1996) EUROPROBE 1996-Lithospheric dynamics: origin and evolution of continents. the EUROPROBE Secretariate, Uppsala University, Uppsala, p 138
- Gorman AR (2002) Ray-theoretical seismic traveltime inversion: modifications for a two-dimensional radially parametrized Earth. *Geophys J Int* 151:511–516
- Grad M, Janik T, Yliniemi J, Guterch A, Luosto U, Komminaho K, Środa P, Höing K, Makris J, Lund CE (1999) Crustal structure of the Mid Polish Trough beneath TTZ seismic profile. *Tectonophysics* 314(1–3):145–160
- Grad M, Keller GR, Thybo H, Guterch A, POLONAISE Working Group (2002) Lower lithospheric structure beneath the Trans-European Suture Zone from POLONAISE'97 seismic profiles. *Tectonophysics* 360:153–168
- Grad M, Jensen SL, Keller GR, Guterch A, Thybo H, Janik T, Tiira T, Yliniemi J, Luosto U, Motuza G, Nasedkin V, Czuba W, Gaczyński E, Środa P, Miller KC, Wilde-Piörko M, Komminaho K, Jacyna J, Korabliova L (2003) Crustal structure of the Trans-European suture zone region along POLONAISE'97 seismic profile P4. *J Geophys Res* 108(B11):2541. <https://doi.org/10.1029/2003JB002426>
- Grad M, Guterch A, Polkowska-Purys A (2005) Crustal structure of the Trans-European Suture Zone in Central Poland: reinterpretation of the LT-2, LT-4 and LT-5 deep seismic sounding profiles. *Geol Q* 49(3):243–252
- Grad M, Guterch A, Keller GR, Janik T, Hegedüs E, Vozar J, Ślaczka A, Tiira T, Yliniemi J (2006) Lithospheric structure beneath trans-Carpathian transect from Precambrian platform to Pannonian basin: CELEBRATION 2000 seismic profile CEL05. *J Geophys Res* 111:B03301
- Grad M, Guterch A, Mazur S, Keller GR, Špičák A, Hrubcová P, Geissler WH, SUDETES 2003 Working Group (2008) Lithospheric structure of the Bohemian Massif and adjacent Variscan belt in central Europe based on Profile S01 from the SUDETES 2003 experiment. *J Geophys Res* 113:B10304. <https://doi.org/10.1029/2007JB005497>
- Grad M, Brückl E, Majdański M, Behm M, Guterch A, CELEBRATION 2000, ALP 2002 Working Groups (2009a) Crustal structure of the Eastern Alps and their foreland: seismic model beneath the CEL10/Alp04 profile and tectonic implications. *Geophys J Int* 177:279–295
- Grad M, Tiira T, ESC Working Group (2009b) The Moho depth map of the European Plate. *Geophys J Int* 176:279–292. <https://doi.org/10.1111/j.1365-246X.2008.03919.x>
- Grad M, Polkowski M, Wilde-Piörko M, Suchcicki J, Arant T (2015) Passive seismic experiment “13 BB Star” in the margin of the East European craton, northern Poland. *Acta Geophys* 63(2):352–373
- Grad M, Polkowski M, Ostaficzuk SR (2016) High-resolution 3D seismic model of the crustal and uppermost mantle structure in Poland. *Tectonophysics* 666:188–210
- Guterch A, Grad M, Materzok R, Perchuc E (1986) Deep structure of the Earth's crust in the contact zone of the Palaeozoic and Precambrian platforms in Poland (Tornquist-Teisseyre Zone). *Tectonophysics* 128:251–279
- Guterch A, Grad M, Janik T, Materzok R, Luosto U, Yliniemi J, Lück E, Schulze A, Förste K (1994) Crustal structure of the transition zone between Precambrian and Variscan Europe from new seismic data along LT-7 profile (NW Poland and eastern Germany). *C R Acad Sci Paris* 319(serie II):1489–1496
- Guterch A, Grad M, Thybo H, Keller GR (1997) POLONAISE'97-International seismic experiment. *Terra Nostra* 11:56–66
- Guterch A, Grad M, Thybo H, Keller GR, POLONAISE Working Group (1999) POLONAISE'97-International seismic experiment between Precambrian and Variscan Europe in Poland. *Tectonophysics* 314:101–121
- Guterch A, Grad M, Keller GR, Posgay K, Vozar J, Spicak A, Brueckl E, Hajnal Z, Thybo H, Selvi O, CELEBRATION 2000 Experiment Team (2003) CELEBRATION 2000 seismic experiment. *Studia Geophys Geod* 47:659–669
- Guterch A, Wybraniec S, Grad M, Chadwick RA, Krawczyk CM, Ziegler PA, Thybo H, Voss WD (2010) Crustal structure and structural framework. In: Doornenbal JC, Stevenson AG (eds) *Petrological geological atlas of the Southern Permian Basin area*. EAGE Publications, Houten, pp 11–23
- Hrubcova P, Środa P, CELEBRATION 2000 Working Group (2008) Crustal structure at the easternmost termination of the Variscan belt based on CELEBRATION 2000 and ALP 2002 data. *Tectonophysics* 460:55–75
- Janik T, Yliniemi J, Grad M, Thybo H, Tiira T, POLONAISE P2 Working Group (2002) Crustal structure across the TESZ along POLONAISE'97 seismic profile P2 in NW Poland. *Tectonophysics* 360:129–152
- Janik T, Grad M, Guterch A, Dadlez R, Yliniemi J, Tiira T, Keller GR, Gaczyński E, CELEBRATION 2000 Working Group (2005) Lithospheric structure of the Trans-European Suture Zone along the TTZ and CEL03 seismic profiles (from NW to SE Poland). *Tectonophysics* 411:129–156. <https://doi.org/10.1016/j.tecto.2005.09.005>
- Janik T, Grad M, Guterch A, CELEBRATION 2000 Working Group (2009) Seismic structure of the lithosphere between the East European Craton and the Carpathians from the net of CELEBRATION 2000 profiles in SE Poland. *Geol Q* 53(1):141–158
- Janutyte I, Majdanski M, Voss PH, Kozlovskaya E, PASSEQ Working Group (2015) Upper mantle structure around the Trans-European Suture Zone obtained by teleseismic tomography. *Solid Earth* 6:73–91. <https://doi.org/10.5194/se-6-73-2015>
- Jensen SL, Janik T, Thybo H, POLONAISE Working Group (1999) Seismic structure of the Palaeozoic Platform along



- POLONAISE'97 profile P1 in NW Poland. *Tectonophysics* 314(1–3):123–144
- Knopoff L, Randall MJ (1970) The compensated linear-vector dipole: a possible mechanism for deep earthquakes. *J Geophys Res* 75:1957–1963
- Komminaho K (1998) Software manual for programs MODEL and XRAYS: a graphical interface for SEIS83 program package. University of Oulu, Department of Geophysics, Report 20, p 31
- Kwiatek G, Martínez-Garzón P, Bohnhoff M (2016) HybridMT: A MATLAB/shell environment package for seismic moment tensor inversion and refinement. *Seismol Res Lett.* <https://doi.org/10.1785/0220150251>
- Lund B (2015) The blast 2015-11-18 (personal communication)
- Lund CE, Prodehl C, Kaminski W, Guggisberg B, Ansorge J (1983) A preliminary interpretation of the long-range seismic refraction profile (Fennolora) through Scandinavia. *Geol Fören Stockh Förh* 105(4):388–388
- Majdański M (2012) The structure of the crust in TESZ area by Kriging interpolation. *Acta Geophys* 60(1):59–75. <https://doi.org/10.2478/s11600-011-0058-5>
- Malinowski M, Żelazniewicz A, Grad M, Guterch A, Janik T, CELEBRATION 2000 Working Group (2005) Seismic and geological structure of the crust in the transition from Baltica to Palaeozoic Europe in SE Poland-CELEBRATION 2000 experiment, profile CEL02. *Tectonophysics* 401:55–77
- Mazur S, Mikolajczak M, Krzywiec P, Malinowski M, Buffenmyer V, Lewandowski M (2015) Is the Teisseyre-Tornquist Zone an ancient plate boundary of Baltica? *Tectonics* 34:2465–2477. <https://doi.org/10.1002/2015TC003934>
- Narkiewicz M, Grad M, Guterch A, Janik T (2011) Crustal seismic velocity structure of southern Poland: preserved memory of a pre-Devonian terrane accretion at the East European Platform margin. *Geol Mag* 148:191–210. <https://doi.org/10.1017/S001675681000049X>
- Pożaryski W, Dembowski Z (1983) Mapa geologiczna Polski i krajów ościennych bez utworów kenozoicznych, mezozoicznych i permskich, 1:1 000 000. Polish Geological Institute, Warsaw (**in Polish**)
- Puziewicz J (2006) Lower crust and uppermost mantle rocks in the area of the Polonaise'97 seismic experiment-petrologic-seismic models. *Prace Państw Inst Geol* 188:53–68 (**in Polish with English summary**)
- Puziewicz J, Polkowski M, Grad M (2017) Geophysical and petrological modeling of the lower crust and uppermost mantle in the Variscan and Proterozoic surroundings of the Trans-European Suture Zone in Central Europe. *Lithos* 276:3–14
- Sethian JA (1996) A fast marching level set method for monotonically advancing fronts. *Proc Natl Acad Sci USA* 93(4):1591–1595
- Sethian JA, Popovici AM (1999) 3-D travelttime computation using the fast marching method. *Geophysics* 64(2):516–523
- Skridlaitė G, Bogdanova S, Page L (2006) Mesoproterozoic events in eastern and central Lithuania as recorded by 40 Ar/39 Ar ages. *Baltica* 19:91–98
- Środa P, POLONAISE Working Group (1999) P and S wave velocity model of the southwestern margin of the Precambrian East European Craton, POLONAISE'97, profile P3. *Tectonophysics* 314(1–3):175–192
- Środa P, Czuba W, Grad M, Guterch A, Tokarski A, Janik T, Rauch M, Keller GR, Hegedűs E, Vozár J, CELEBRATION 2000 Working Group (2006) Crustal structure of the Western Carpathians from CELEBRATION 2000 profiles CEL01 and CEL04: seismic models and geological implication. *Geophys J Int* 167:737–760. <https://doi.org/10.1111/j.1365-246X.2006.03104.x>
- Wessel P, Smith WHF (1995) New version of generic mapping tools released. *EOS* 76:453
- Wiejacz P (1991) Investigation of focal mechanisms of mine tremors by the moment tensor inversion, Ph. D. Thesis. Institute of Geophysics, Polish Academy of Sciences Warsaw (**in Polish**)
- Wilde-Piórko M, Geissler WH, Plomerova J, Grad M, Babuska V, Bruckl E, Cyziene J, Czuba W, England R, Gaczyński E, Gazdova R, Gregersen S, Guterch A, Hanka W, Hegedus E, Heuer B, Jedlicka P, Lazuskiene J, Keller GR, Kind R, Klinge K, Kolinsky P, Komminaho K, Kozlovskaya E, Kruger F, Larsen T, Majdański M, Malek J, Motuza G, Novotny O, Pietrasiak R, Plenefisch Th, Ruzrk B, Sliupa S, Środa P, Świeczak M, Tiira T, Voss P, Wiejacz P (2008) PASSEQ 2006-2008: Passive seismic experiment in Trans-European Suture Zone. *Studia Geophys Geod* 52:439–448. <https://doi.org/10.1007/s11200-008-0030-2>
- Wilde-Piórko M, Świeczak M, Grad M, Majdański M (2010) Integrated seismic model of the crust and upper mantle of the Trans-European Suture zone between the Precambrian craton and Phanerozoic terranes in Central Europe. *Tectonophysics* 481:108–115. <https://doi.org/10.1016/j.tecto.2009.05.002>
- Winchester JA, The PACE TMR Network Team (2002) Palaeozoic amalgamation of Central Europe: new results from recent geological and geophysical investigations. *Tectonophysics* 360:5–21
- Zelt CA (1994) Software package ZPLOT. Bullard Laboratories, University of Cambridge, Cambridge
- Zelt CA (1999) Modelling strategies and model assessment for wide-angle seismic travel-time data. *Geophys J Int* 139:183–204
- Ziegler PA (1990) Geological atlas of western and central Europe, 2nd ed. Shell International Petroleum Maatschappij, Hague, Geological Society Publishing House, London